CHAPTER V
PREPARATION AND CHARACTERIZATION OF POLYAMIDE6/BACTERIAL NANOCOMPOSITE FILMS

5.1 Abstract

The flexible piezoelectric films of polyamide 6 (PA6)/bacterial cellulose (BC) were prepared via solution casting and casted by compression method as a thin films. The weight percentage of extracted BC at 1wt% was incorporated into PA6 matrix using formic acid as a solvent. The results showed that higher amount of BC can slightly increase thermal stability, crystallinity and mechanical properties of the nanocomposite, but it made the composite less transparent. The tensional behavior of nanocomposite films was improved compared with neat PA6, Young's modulus was increased from 1011 to 1093Mpa at 1wt% of BC. Inclusion of BC additionally increase dielectric and piezoelectric properties due to the interfacial polarization that might be generated at the interfaces between fiber and polymer matrix.

5.2 Introduction

From PA11/BC nanocomposite results, These nanocomposite films show increased as increasing BC content. Young's modulus of nanocomposite films were higher than neat PA11 as increasing BC content. BC has effects on PA11 crystallinity (X_C) but has no effect on T_m and T_d. The storage modulus of the nanocomposite films was higher than neat PA11. The partially interactions between the interface of BC and PA11 yield to enhance of dielectric properties and the poling process can cause the dielectric constant tend to increase. However, for the optical property, the incorporated of BC decreased the percentage of transmittance in all visible light range. So, The 1wt% of BC was chosen to further study the PA6 on the relate properties with basis of piezoelectric touch sensor due to highest percentage of transmittance compare with other compositions, moderate storage modulus, moderate dielectric constant and lowest dissipation factor at any temperature and frequency.

5.3 Experimental Procedures

5.3.1 Materials

Nata de coco was purchased from local food market. PA6 was purchased from BASF Co., Ltd. Formic acid (AR grade, 99%) and sodium hydroxide (NaOH) (AR grade, 98%) were purchased from S.M. Chemical Co., Ltd. And Labscan Ltd., respectively.

5.3.2 BC preparation (Pakdeepatarapun *et al.*, 2014)

Nata de coco gel was firstly washed with water to remove some excess sugar. After that the washed nata de coco gel was grinded and treated with 0.1 M NaOH at 80 °C for 2 h to obtain the BC pellicles. The BC pellicles were then washed with hot deionized water until neutral pH is reached. The BC pellicles were dispersed in deionized water and kept in bottle.

5.3.3 Fabrication of PA6/BC Nanocomposite Films

BC paste was rinsed with formic acid to remove all water content. Then BC dispersed in formic acid was obtained. Polyamide 6 dissolved in formic acid is mixed with BC dispersed in polyamide with the percentage weight at 1wt%. Then the mixture solution was mixed by mechanical stirrer and taken into the ultrasonic bath to obtain better dispersion for an hour. The mixture solution will be further dropped into clean cool water for 10 minutes. After that they are heated in vacuum oven at 70 °C for 2 days. The blend will be obtained., the casted blend films were obtained. Finally, the casted film were performed by a compression press (Wabush, model No.V50H-15-RPX, 4-post design) with preheating for 5 min, followed by compressing for 5 min at 5 Tons. The operating temperature of mold was maintained at 250 °C.

5.3.4 Characterizations

The morphology of BC samples were observed through transmittance electron microscope (TEM, JEOL-2100). The thermal properties were investigated by differential scanning calorimeter (DSC, METTLER, DSC822) and thermal

gravimetric analyzer (TGA, Perkin Elmer). X-rays diffraction microscope (XRD, Rigaku, model Dmax 2002) were used to determine crystalline phases of the nanocomposite films. Tensile properties were investigated follow the ASTM D882. The optical property was determined by using UV/Vis spectrophotometer (Shimadzu 2550). The dielectric constant and dissipation factor were measured using a Network Analyzer (Agilent, E4991A).

5.4 Results and Discussion

5.4.1 PA6/BC nanocomposite Films Characterization

5.4.1.1 Morphological Properties

Figure 5.5 shows a cross-sectional SEM images of PA6/BC compared with neat PA6 at the magnification of 1 k. With the amount of BC content at 1wt%, the toughness of the blend film tended to be decreased which can be confirmed by the sample's surface fracture. The fiber in Figure 5.5 shows that BC was pulled out from PA6 matrix that indicated the interaction between PA11 and BC is good because BC was stick on PA6 matrix.

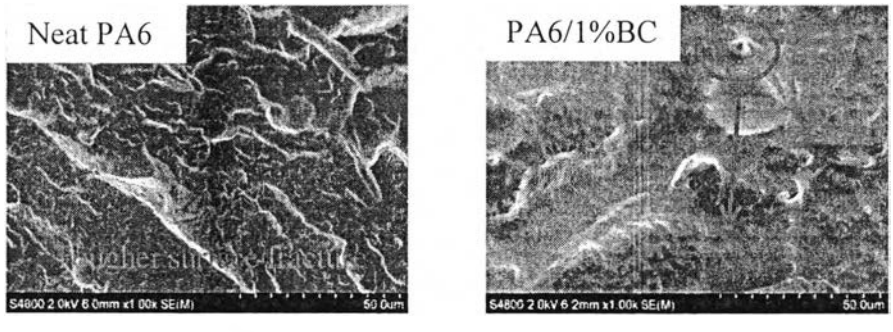

Figure 5.1 SEM images of PA6/BC blend films at different weight compositions at magnification of 1 k.

5.4.1.2 Crystalline Phase Behavior

Figure 5.6 shows that PA6 has 2 types of stable crystalline forms, monoclinic α-crystalline form and monoclinic γ-crystalline form. The peak appeared at around $2\theta = 20^{\circ}$ and 24.8 ° were α-crystalline form which was (200) and

(002) plane respectively. The peak at around 2θ = 21.4 ° was γ-crystalline form. For PA6/BC1%wt nanocomposites, with increasing BC content, the diffraction intensity of γ was decreased. When BC content was 1wt%, a sharp diffraction peak appeared at 2θ = 20° and 24.8 °. Based on this figure, we can predict that BC can increase α-crystalline form of PA6 (Jiang, T. *et al*, 2005).

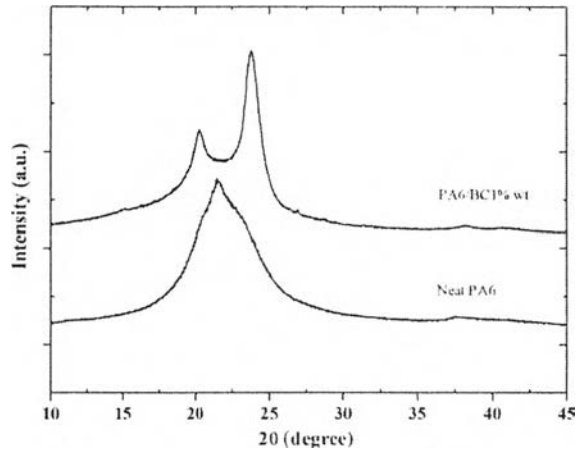

Figure 5.6 X-ray diffraction patterns of PA6/BC nanocomposite films compared with neat PA6.

5.4.1.3 Thermal Properties

Thermal degradation behavior of PA6/BC nanocomposite film was measured by using TGA. Figure 5.7 Shows TGA thermogram of nanocomposite at 1 wt% of bacterial cellulose compared with neat PA6. The result showed that the degradation started at 350°C which referred to degradation temperature of PA6 and the result demonstrated that bacterial cellulose had no effect to improve the thermal stability of PA6 polymeric chain. The nanocomposite films were free from formic acid due to the absence of thermal degradation at 100.8 °C, which was the boiling point of formic acid.

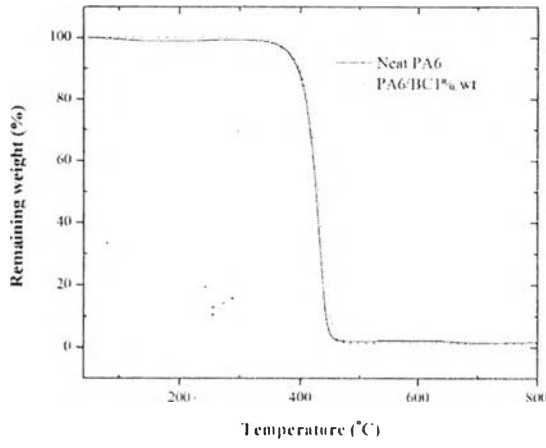

Figure 5.3 TG-DTA thermograms of PA6 nanocomposite films.

The DSC parameters are shown in Table 5.1. From the result, there was one transition temperature observed at 218 °C and 191 °C which corresponding to T_m and T_c of PA6. Figure 5.8 shows the second-heating curves of PA6/BC nanocomposite films. BC has effects on crystallinity (X_C) but has no effect on T_m and T_c. The results show that increasing of BC content at 1 wt% can slightly increase X_C, this may occur due to orientation and dispersion of BC resulted to higher possibility of PA6 chains to come close and crystallize. The crystallinity temperature are showed in Figure 5.10, indicate that higher amount of BC can shift T_c higher because the nanocomposite films need higher energy to crystallize with the presence of BC.

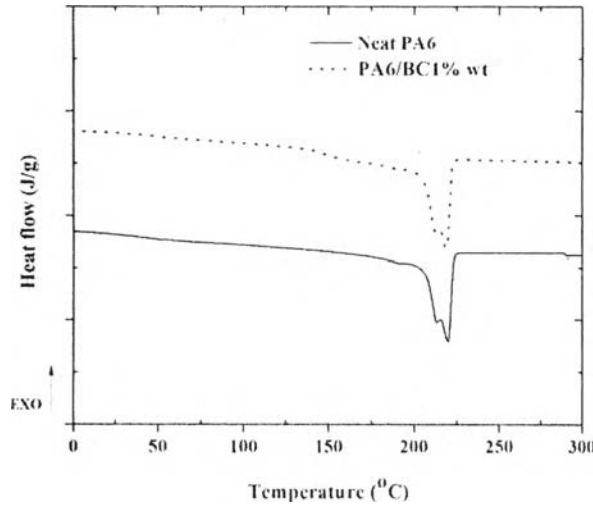

Figure 5.4 DSC second-heating curves of PA6/BC nanocomposite films.

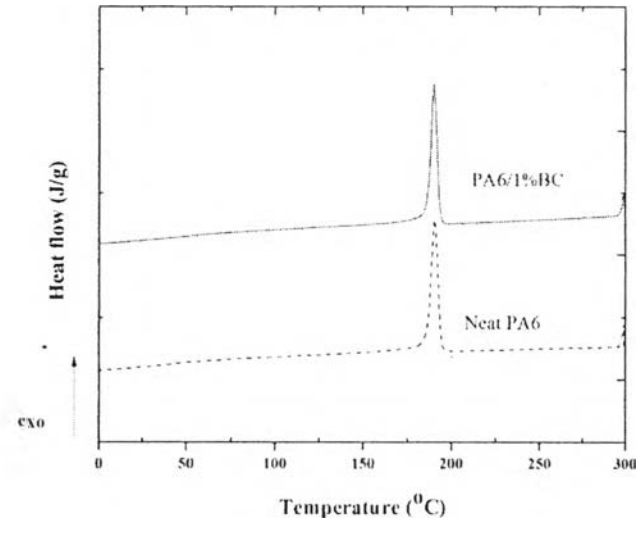

Figure 5.5 DSC first-cooling curves of PA6/BC nanocomposite films.

Table 5.1 DSC parameters of PA6/BC mamocomposite films compared with neat PA11

Sample	ΔH_m (J/g)	T_m (°C)	X_c (%)	T_c (°C)
Neat PA6	74.8	218	32.6	191.1
PA11/1%BC	78.9	219	34.3	190.6

*Heat of fusion value for 100% crystalline PA11, ΔH_m^o = 230.1 J/g

5.4.1.4 Mechanical Properties

With the incorporation of BC, the nanocomposite films become more brittle as can be seen in Figure 5.12 which corresponded to SEM images in figure 5.5 that showed the tough surface fracture. Figure 5.10, BC provided slightly higher Young's modulus to the nanocomposite films compared with neat PA6.Moreover, BC provided the higher tensile strength of the nanocomposite as can be seen in Figure 5.11 which corresponded to SEM images that show the interaction between polymer matrix and filler in films that make the tensile strength increased.

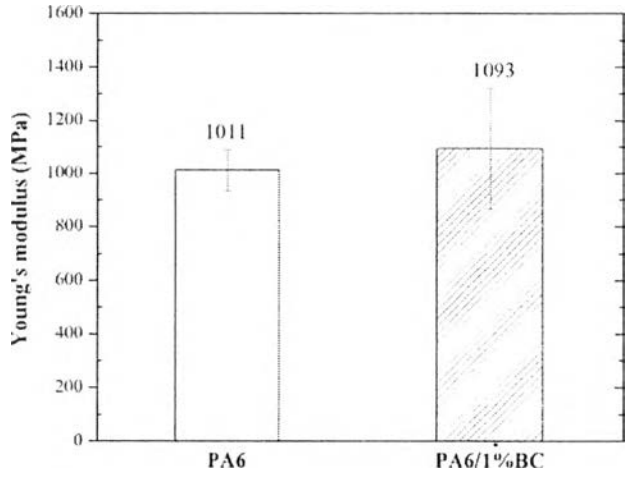

Figure 5.6 Young's modulus of PA11/BC nanocomposite films.

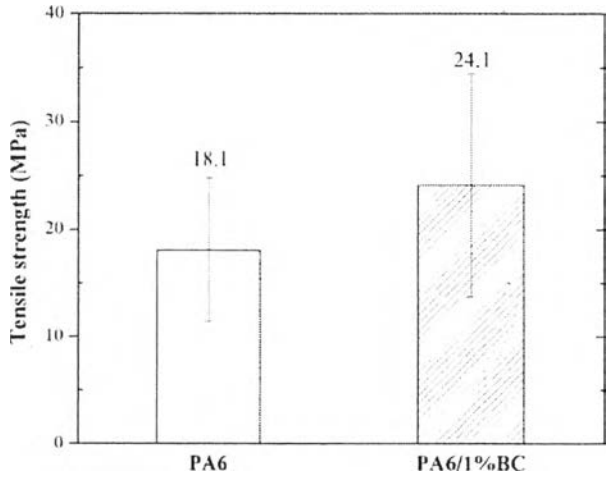

Figure 5.7 Tensile strength of PA11/VC nanocomposite films.

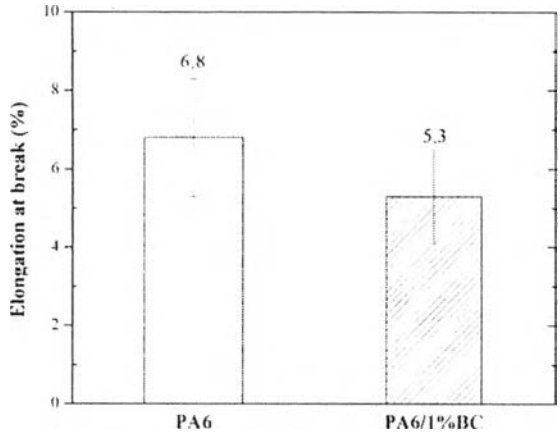

Figure 5.8 Elongation at break of BC/PVDF blend films.

5.4.1.5 Optical Properties of PA6/BC Blend Films

Figure 5.13 which shows UV/Vis spectra of the neat PA6 and PA6/BC nanocomposite films and reference is air. Neat PA6 has 10-20% transmittance in the visible light region (500-800 nm), when adding BC, the transmittance slightly decrease, which means BC exhibits the opacity property. It is due to the crystallization of nanocomposite films because PA can form crystal quickly after compression process and from crystalline results, BC can act as a nucleating agent that made the transmittance tend to decrease.

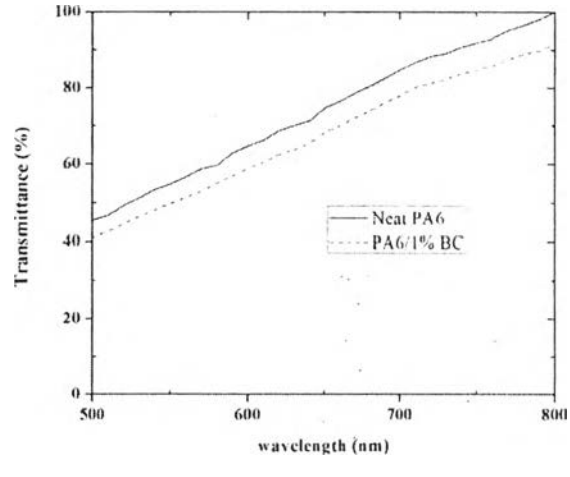

Figure 5.9 UV/Vis spectra of PA6/BC nanocomposite films compared with neat PA6.

5.4.2.6 Dielectric Properties of PA6/BC nanocomposite Films

The dielectric constant related to piezoelectric properties via the equation "$d_{ij} = \varepsilon_{ii} g_{ij}$" , where d_{ij} is stress piezoelectric coefficient, ε_{ii} is the permittivity of the material and g_{ij} is strain piezoelectric coefficient and ε_o is the vacuum dielectric constant permittivity (8.85×10^{-12} F/m). This equation shows that the dielectric property is a basis property for piezoelectric materials. In this part, the effect of frequency, temperature and BC content on dielectric behavior of PA6/BC nanocomposite films and neat PA6 were discussed.

Figure 5.14 shows dielectric constant (a) and dissipation factor (b) of neat PA6 and PA6/BC nanocomposite films at 1 wt% of BC loading as a function of frequency (10 MHz - 1 GHz) at room temperature. Compared to neat PA6, adding with 1 wt% BC exhibited higher dielectric constant because BC can induced the interfacial polization of PA causing higher dielectric constant. For dissipation factor on frequency dependent, dissipation factor slightly decreases with increasing frequency.

This increasing occurred due to the interfacial polarization between the hydroxyl group in the BC chain and amide group in PA chain, higher amount of polar hydroxyl group in BC, and the higher dielectric constant of nanocomposite films. Moreover, a higher content of BC in the films caused higher water content, which increased dissipation factor of films.

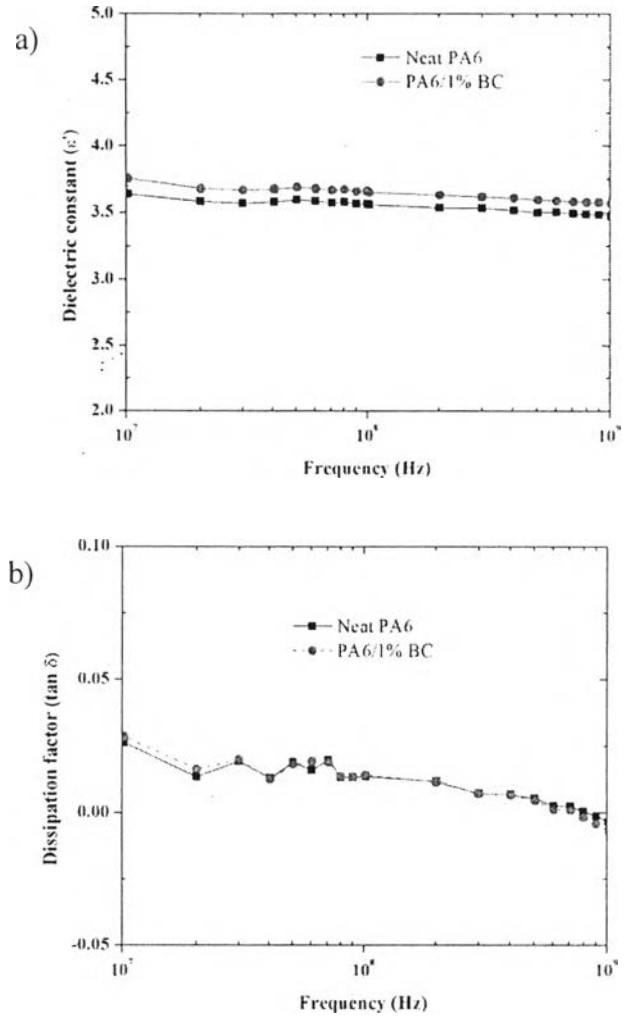

Figure 5.10 Dielectric constant (a) and dissipation factor (b) of PA6 and PA6/BC mamocomposite films as a function of frequency at 20°C.

5.5 Conclusion

Polyamide6 (PA6) was mixed with bacterial cellulose (BC) by using solution casting method using formic acid as solvent. Then casted nanocomposite films were prepared by hot-compressed method. The TEM images indicated that BC has nano-scale diameter around 30-50 nm formimg a network structure which yield to high surface area and create more intermolecular interaction between hydrogen atoms and amide bonds. These nanocomposite films show that there was phase of monoclinic α-phase crystallinity that was increased as increasing BC content. Young's modulus of nanocomposite films were higher than neat PA6 as increasing

BC content. BC has effects on PA6 crystallinity (X_C) but has no effect on T_m, T_c and T_d.

In addition, there was also the chemical attraction between hydroxyl group in BC structure and nitrogen atom in PA6 chain. These interactions can be observed from the SEM images. The partially interactions between the interface of BC and PA6 yield to enhance of dielectric properties of PA6/BC nanocomposite but BC enhance dielectric properties of PA11/BC nanocomposite more than PA6/BC nanocomposite at same content due to the structure of odd-numbered PA. However, for the optical property, the incorporated of BC decreased the percentage of transmittance in all visible light range.

5.6 Acknowledgement

This work has partially been supported by the Petroleum and Petrochemical College, Chulalongkorn University.

References

Bak, H., Cho, S.Y., Yun, Y.S., Jin, H.J., (2010). Electrically conductive transparent films base on nylon 6 membranes and single-walled carbon nanotube. Current Applied Physics, 10, 468-472.

Balasubramanian, V., Kelkar, D.S., Kurup, M.B., (1996). Electric conduction in ion implanted nylon-6 films. Nuclear Instruments and Methods in Physics Research B, 113, 257-260

Bhavna, V.M., Patil, S.V. (2014). Physical, structure, mechanical and thermal characterization of bacterial cellulose by G. hansenii NCIM 2529. Carbohydrate Polymers, 106, 132-141.

Czaja, W., Krystunowicz, A., Bielecki, S., Brown Jr., R.M. (2006). Microbial cellulose-the natural power to heal wounds. Biomaterials, 27, 145-151.

Fukada, E. (2000). History and recent profress in piezoelectric polymers. IEEE Transactions on Ultrasonics, Ferroelectrics, and Frequency Control, 47(6), 1277-1290.

Gang, W., Yano, O., Soen, T. (1985). Dielectric and piezoelectric properties of nylon 9 and nylon 11. Polymer Journal, 18(1), 51-61.

Harrison, J.S. and Z. Ounaies (2001). Piezoelectric Polymers. ICASE. Virginia: National Aeronautics and space Administration.

Jiang, T., Wang, Y., Yeh, J., Fan, Z. (2005). Study on solvent permeayion resistance properties of nylon6/clay nanocomposite. European Polymer Journal, 41, 459-466.

Miri, V., Persyn, O., Lefebvre, J.M., Seguela, R. (2009). Effects of water absorption on the plastic deformation behavior of nylon 6. European Polymer Journal, 45, 757-762.

Nasrullah, S., Ul-Islam, M., Khattak, W.A., Park, J.K. (2013). Overview of bacterial cellulose composites: A multipurpose advanced material. Carbohydrate Polymers, 98, 1585-1598

Nogi, M., Yano, H. (2008). Transparent nanocomposites based on cellulose produced by bacterial offer potential innovation in the electronic device. Advanced Materials, 20(10), 1848-1852

Page, I.B. (2000). Polyamide as engineering thermoplastic materials. Rapra Review Reports. Poland: Rapra Technology LTD.

Peter, F., Kreammer, A., Neumann, W., Gerhard-Multhaupt, R. (2004). Dielectric relaxation in piezo-, pyro- and ferro electric polyamide 11. IEEE Transactions in Dielectrics and Electrical Insulation, 11(2), 271-279.

Peter, F.V., Cardona. T.D., Nout, M.J.R., Gooijer, K.D.D., Heuvel, J.C.V.D. (2000). Location and limitation of cellulose production by acetobactor xylinum established from oxygen profiles. Journal of Bioscience and Bioengineering, 89(5), 414-419.

Ramona-Daniela, P., Stoica-Guzun, A., Stroescu, M. (2014). Composite films of poly(vinyl alcohol)-chitisan-bacterial cellulose for drug controlled release. International Journal of Biological Macromolecules, 68, 117-1240.

Sampson, K.A., Mishra, A.K., Waghmare, U.V. (2012). Dielectric and piezoelectric responses of nylon-7: A first-principles study. Journal of Polymer, 53(2751-2757).

Takase, Y., Lee, J.W., Scheinbeim, J.I., Newman, B.A. (1991). High-temperature characteristic of nylon-11 and nylon-7 piezoelectrics. Macromolecules, 24, 6644-6652.

Thi, T.N., Sugiyama, J., Bulone, V. (2010). Bacterial cellulose-based biomimetic composite. Biopolymer. Hirishima: Biomass Technology Research Centre, National Institute of Advanced Industrial Science and Technology.

Tulsyan, K. (2007). Amorphous polyamide nanocomposite: Effects of Stability of The Nanoclay Modifier. Massachusetts: Department of Plastic Engineering, University of Massachusetts Lowell.

Ul-Islam, M., Khan, T., Park, J.K. (2012). Nanoreinforced bacterial cellulose-montmorillonite composites for biomedical applications. Carbohydrate Polymer, 89, 1189-1197.

Ul-Islam, M., Khan, T., Park, J.K. (2012). Water holding and release properties of bacterial cellulose obtained by in situ and ex situ modification. Carbohydrate Polymers, 88, 596-603.

Vijaya, M.S. (2013). Applications in engineering and medical sciences, Piezoelectric Materials and Devices. New York: Taylor and Francis Group.

Yanhuai, D., Zhang, P., Jiang, Y., Xu, F., Yin, J., Zuo, Y., (2009). Mechanical properties of nylon-6/SiO_2 nanofiber prepared by electrospining. Materials Letters, 63, 34-36.

Zhang, Q., Mo, Z., Zhang, H., Liu, S., Cheng,S., (2001). Crystal transitions of nylon11 under drawing and annealing. Polymer, 42, 5543-5547.